Article

Not peer-reviewed version

Evaluation of Novel Nasal Mucoadhesive Nanoformulations Containing Lipid-Soluble EGCG for Long COVID Treatment

Nicolette Frank , Douglas Dickinson , Garrison Lovett , Yutao Liu , Hongfang Yu , Jingwen Cai , Bo Yao , Xiaocui Jiang , Stephen Hsu *

Posted Date: 30 April 2024

doi: 10.20944/preprints202404.1974.v1

Keywords: Respiratory virus; Long COVID; Nasal drug; EGCG-palmitate; Nanoformulations

 doi:10.20944/preprints202404.1974.v1

Article

Evaluation of Novel Nasal Mucoadhesive Nanoformulations Containing Lipid-Soluble EGCG for Long COVID Treatment

Nicolette Frank [1], Douglas Dickinson [2], Garrison Lovett [1], Yutao Liu [1], Hongfang Yu [1], Jingwen Cai [1], Bo Yao [3], Xiaocui Jiang [3] and Stephen Hsu [1,2,*]

[1] Augusta University, Augusta,
[2] Camellix Research Laboratory, Augusta, GA
[3] Hangzhou Shanju Biotech Co., Ltd. Hang Zhou, China.
* Correspondence: shsu@augusta.edu; Tel.: 01-706-721-4816

Abstract: Neurologic symptoms associated with Long COVID result from the persistent infection of SARS-CoV-2 in the nasal neuroepithelial cells, leading to inflammation in the central nervous system (CNS). As of today, there is no evidence that vaccines or medications can clear the persistent viral infection in the olfactory mucosa. Recently published clinical data demonstrate that only 5% of Long COVID anosmia patients have fully recovered during the past 2 years and 10.4% of COVID patients are still symptomatic 18 months post infection. Our group demonstrated that epigallocatechin-3-gallate-monopalmitate (EC16m) nanoformulations possess strong antiviral activity against human coronavirus, suggesting this green tea-derived compound in nanoparticle formulations could be developed as an intranasally delivered new drug targeting the persistent SARS-CoV-2 infection, as well as inflammation and oxidative stress in the CNS, leading to restoration of neurologic functions. The objective of the current study is to evaluate the mucociliary safety of the EC16m nasal nanoformulations and the efficacy against human coronavirus. Methods: nanoparticle size and Zeta potential were measured using the ZetaView Nanoparticle Tracking Analysis system; mucociliary safety was determined using MucilAir Human Nasal Epithelium Model; contact antiviral activity and post-infection inhibition against OC43 viral strain were assessed by TCID50 assay for cytopathic effect on MRC-5 cells. Results: the saline-based EC16 mucoadhesive nanoformulations containing 0.005 to 0.02% w/v EC16m have no significant difference in comparison to saline (0.9% NaCl) on tissue integrity, cytotoxicity, and cilia beat frequency. A 5-minute contact inactivated 99.9% of the β-coronavirus OC43. OC43 viral replication was inhibited by >99% after infected MAR-5 cells were treated with one of the formulations. Conclusion: the saline-based novel EC16m mucoadhesive nasal nanoformulations rapidly inactivated human coronavirus with mucociliary safety measurements comparable to saline, a solution widely used for nasal applications.

Keywords: respiratory virus; long COVID; nasal drug; EC16; EGCG-palmitate; nanoformulations

1. Introduction

According to Center of Disease Control and Prevention (CDC), Long COVID symptoms can last weeks, months, or years after COVID-19 illness and can sometimes result in disability (CDC, Long COVID or Post-COVID Conditions). The neurologic symptoms associated with Long COVID include fatigue, 'brain fog', cognitive impairment, headache, sleep, mood, smell, or taste disorders, myalgias, sensorimotor deficits, dizziness, anxiety, depression, earache, hearing loss, and/or ringing in the ears, dysautonomia, and psychiatric manifestations [1–3]. The pathogenesis of these Long COVID neurologic symptoms involves neuroinvasion of SARS-CoV-2 from the nasal neuroepithelium to the support and stem cells in the olfactory mucosa, causing persistent olfactory dysfunction (anosmia).

 doi:10.20944/preprints202404.1974.v1

The persistent presence of SARS-CoV-2 also induces dysregulation of innate and adaptive immunity with prolonged cytokine release, oxidative stress, lymphocytic infiltration in the central nervous system (CNS), leading to neurodegeneration and tress, and neurodegeneration and demyelination [4]. Thus, therapeutic approaches targeting Long COVID neurologic symptoms must address the persistent presence of SARS-CoV-2. Effort has been taken to reduce the neurologic symptoms using antiviral drug such as Nirmatrelvir (oral), and steroids like fluticasone (nasal), mometasone (nasal), and naltrexone (oral). Among these clinical studies, the only randomized double-blind clinical trial showed mometasone nasal spray did not have significant improvement in recovery rates and duration of anosmia [5]. A Phase II clinical trial using nasal irrigation with saline + 400 mg theophylline in Long COVID patients did not generate satisfactory outcomes [6]. In order to address the "root cause" of Long COVID neurologic symptoms, the best approach is to simultaneously reduce the persistent SARS-CoV-2 viral presence (persistent infection), inflammation of olfactory epithelia, oxidative stress and damage in the CNS [7].

Based on our recent studies, we hypothesized that epillagocatechin-3-gallate (EGCG)-mono-palmitate (EC16m), a compound with multi-mechanisms of antiviral activity, plus anti-inflammatory, antioxidant, and neuroprotective properties, has potential to become a new nasal drug to minimizing Long COVID associated neurologic symptoms such as anosmia [8,9].

EGCG is a hydrophilic naturally formed major green tea polyphenol, which has a wide spectrum of antiviral activity [10,11], including SARS-CoV-2 [12]. The mono-palmitoylated EGCG (EC16m) is also a naturally-occurring green tea catechin but EC16m is an amphipathic compound [13]. We have shown that EC16m is able to enter epithelial cells and hydrolyzed by esterase in the cytoplasm, releasing free EGCG [13,14]. Conversely, EGCG can be esterified chemically to EC16m as illustrated below [15].

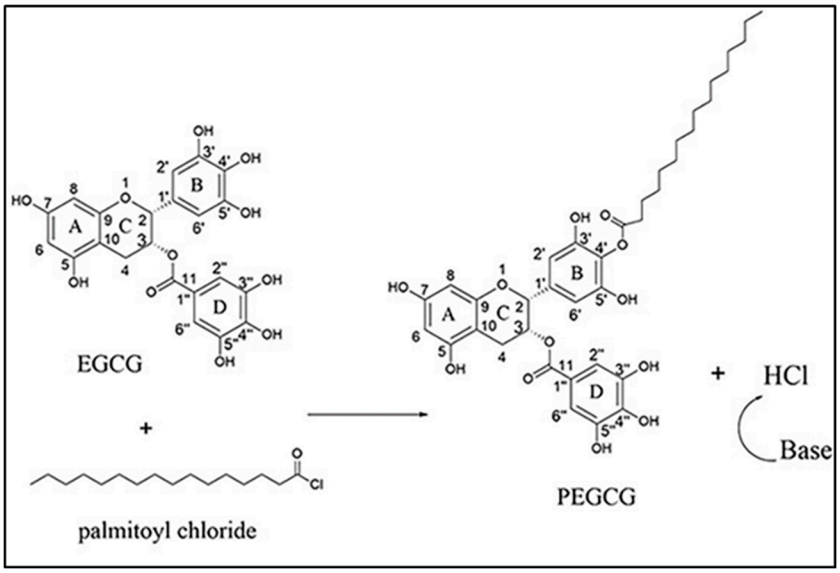

Schematic esterification of EGCG to form EGCG-4'mono-palmitate (EC16m) [15].

In addition to its antiviral properties, EGCG is able to reduce epithelial cell inflammation in vitro and in vivo [16]. In autoimmune animal studies, we found that EGCG significantly reduced lymphocyte infiltration and serum autoantibody levels, and protects human cells from TNF-α-induced cytotoxicity [17,18]. Interestingly, our animal studies showed that EGCG modulates the antioxidant defense enzymes to protect cells from free radical-induced damage [19] and stabilizes p21 expression and reduces DNA damage from inflammation-induced reactive oxygen species [20]. Also, it has been widely reported that EGCG provides neuroprotective effects in preclinical studies and clinical trials [21–23]. However, poor bioavailability and instability of EGCG prevent its beneficial effects to be realized in new drug development [15,24–27].

In comparison to water-soluble EGCG, EC16m is significantly more potent against influenza virus, herpes simplex virus, and norovirus [26,28,29]. Our recent studies demonstrate nanoparticles

 doi:10.20944/preprints202404.1974.v1

of EC16 (contains 50% EC16m) or EC16m in saline-based nasal formulations are able to rapidly inactivate human coronavirus [30,31].

The invention of a "facilitated self-assembling" method to generate nanoparticles of the amphipathic compound EC16/EC16m is a milestone in nanotechnology (U.S. Application No. 63/490,712), which enables us to formulate aqueous suspensions of the nanoparticles for various purposes, especially in disease control and prevention using highly effective and natural compounds. The EC16 nanoparticles (NPs) do not belong to any currently classified NPs such as incidental, bioinspired, anthropogenic, or engineered NPs [30].

Attempts at making green tea catechin (polyphenol) NPs have been explored with different methods. For example, lipid-based NPs of EGCG were produced with different lipids and a surfactant, and evaluated for potential use in cancer treatment through oral administration [31–33]. EGCG can be encapsulated in hordein NPs [34], and further coated with chitosan [35] to improve the bioavailability of EGCG [36].

Unlike other engineered EGCG NPs, the EC16/EC16m NPs were made through a "facilitated self-assembling" method (proprietary, patent pending), which does not involve association with metals, monomers, oil, or encapsulation. In addition to the high efficacy of rapid inactivation of human coronavirus OC43 and 229E, the water-based nanoformulations are not associated with cytotoxicity [8,9]. In contrast, recently published data showed that engineered EGCG-AgNPs appears cytotoxic to human skin cells (CC50 =30 μg/mL), and the efficacy is poor on human herpes simplex virus type 1 and type 2, with less than $\log_{10}$ 2 reduction (<99%) after 60 min incubation [37]. Another study indicated that EGCG-AgNPs have been shown to become cytotoxic at nM levels [38], while EC16 NPs at 1.4 mM is not associated with cytotoxicity [9].

For intranasally applied formulations, nasal mucociliary clearance transit time (MCCTT) and mucociliary toxicity must be considered. The previously tested saline-based aqueous EC16m nanoformulations need to be further formulated to a mucoadhesive formulation because the human MCCT is under 20 min [39]. These novel EC6m mucoadhesive nanoformulations should possess rapid antiviral effect without mucociliary toxicity. The objectives of the current study is to evaluate the mucociliary safety of the EC16m nasal nanoformulations using a 3D Human Nasal Epithelium Model (MucilAir) and test the efficacy against human β-coronavirus OC43.

2. Materials and Methods

2.1. Virus and Cell Lines

OC43 human β-coronavirus (ATCC VR-1558), HCT-8 human epithelial cells (ATCC HRT-18), and MRC-5 human respiratory fibroblast cells (ATCC CCL-171) were purchased from ATCC (Manassas, Virginia, USA). HCT-18 cells were used in cell viability (MTT) assays. MRC-5 cells were used for antiviral assays on OC43 virus.

2.2. EC16m and Other Supplies

Epigallocatechin-3-Gallate-4' mono-palmitate (EC16m, CAS# 507453-56-7), was provided by Camellix, LLC (Evans, GA, USA). Dulbecco's Modified Eagle's Medium (DMEM) was purchased from ATCC (30-2002). Trypsin-EDTA Solution was purchased from ATCC (30-2101). Fetal bovine serum (FBS) was from Neuromics (Edina, MN, USA). Penicillin, streptomycin, and amphotericin B solution (100x) was obtained from Corning (Glendale, AR, USA). Carboxymethylcellulose (CMC) was from Fisher Scientific (Waltham, MA). Plasticwares were purchased from Southern Labware (Cumming, GA, USA).

2.3. EC16 Mucoadhesive Nanoformulations

EC16m (formula weight 697) nanoparticles were initially dispersed in 90% glycerol as stable stocks at 1% w/v using a facilitated self-assembling method (proprietary). This EC16m nanoparticle stock was further diluted with Normal Saline (0.9% NaCl) to final formulations containing 0.005 (70 μM) to 0.02% (280 μM), 0.5% carboxymethylcellulose (CMC), with or without a food-grade

 doi:10.20944/preprints202404.1974.v1

dispersing agent (proprietary). The nanoformulations with the dispersing agent have a pH of 6.22 and viscosity at 19 mPa. The nanoformulations without the dispersing agent have a pH of 6.21 and viscosity of 14 mPa.

2.4. Evaluation of Particle Size Distribution (Detailed Data Sheets Are in Appendix A)

ZetaView nanoparticle tracking analysis was performed according to a method described previously [9,40]. The particle size distribution and concentration were measured using the Zetaview x20 (Particle Metrix, Meerbusch, Germany) and corre-sponding software. The measuring range for particle diameter is 10-2000 nm. These samples were diluted by the same volume of 1×PBS and then loaded into the cell. Particle information was collected from the instrument at 11 different positions across the cell, with two cycles of readings respectively. Standard operating procedure was set to a temperature of 23°C, a sensitivity of 70, a frame rate of 30 frames per second, and a shutter speed of 100. The post-acquisition parameters were set to a minimum bright-ness of 20, a maximum area of 1000, a minimum area of 10, and the trace length of 15 [40].

2.5. Evaluation of Cytotoxicity by Cell Viability (MTT) Assay

HCT-8 cells were allowed to form a monolayer in 96-well plates prior to incubation with the nanoformulations (Formulations A, B, C and D) and control formulations (Normal saline) in a series of dilutions for 60 min. The testing nanoformulations were replaced with DMEM medium with 10% FBS and incubated overnight. The MTT assay was performed the next day using CytoSelect MTT Cell Proliferation Assay kit (Cell Biolabs, Inc, San Diego, CA, USA) according to the method provided by the manufacturer.

2.6. Evaluation of Mucociliary Toxicities of EC16m Nanoformulations by 3D MucilAir Human Nasal Epithelium Model (Performed by Epithelix Sàrl, Plan-les-Ouates Switzerland. Detailed Protocols Are in Appendix B)

The aim of this evaluation was to study the acute mucociliary toxicological effect of EC16m nasal spray nanoformulations using fully differentiated human nasal epithelial cells cultured at the air-liquid interface. Human nasal epithelia (MucilAir™-Pool) was reconstituted with a mixture of cells isolated from 14 different normal nasal donors. Formulations A, B, C and D (FA, FB, FC, and FD) were exposed apically for 2 days. At time 0 (day 1), 10 µl of the nanoformulation were applied apically twice a day during 30 minutes with 6 hours interval on MucilAir™- Pool inserts. On day 2, apical applications were applied twice during 30 minutes with 6 hours interval. Subsequently, tissue integrity (TEER), Lactate dehydrogenase (LDH) release (cytotoxicity) and cilia beating frequency (CBF) were measured at the end of the experiment. Detailed protocols are presented as appendices. The experiments were repeated three times in Epithelix laboratories. Normal saline (0.9% NaCl) was used as vehicle control. 10% Triton X in the culture medium was used as positive control.

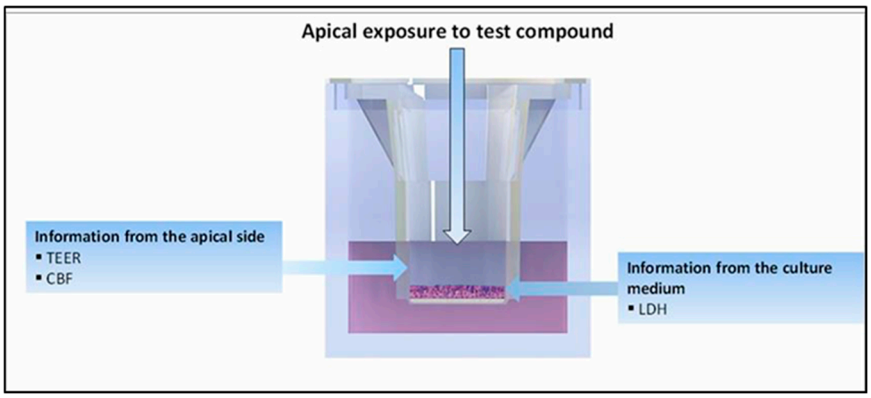

Figure 1. Schematic illustration of sample application and end-point measurements of MucilAire 3D human nasal model.

 doi:10.20944/preprints202404.1974.v1

2.7. Direct Contact Antiviral Activity Tests

Infection of cells by OC43 virus, and viral titer: MRC-5 cells were cultured in DMEM Medium supplemented with 10% FBS and 1% penicillin, streptomycin, and amphotericin B. The viral infection assay and viral titering were performed in 96 well cell culture plates when the cells had reached 90% confluency. A 10-fold series dilution of OC43 virus in DMEM containing 2% FBS (MM) was loaded into wells in quadruplicates per dilution. After a one-hour absorption, the viral dilutions were removed and 100 µl MM was added, followed by incubation at 33oC with 5% CO2 for >4 days to allow a CPE (cytopathic effect) to become visible. Viral titer was calculated by a TCID50 Excel software based on Reed–Muench Method [41]. A minimum of three independent experiments were performed and results recorded.

2.8. Post-Infection Test

To test if EC16m nasal nanoformulations possess a post-infection effect, MRC-5 cells were allowed to form a monolayer (90% confluent) in a 96-well cell culture plate prior to a one-hour infection of OC43 virus in a series dilution to 10^{-9} before removal of virus. Then, 50 µl of EC16m nanoformulation were applied to the designated wells for 5 min before being replaced by MM. The vehicle control wells were treated with the vehicles after viral infection for 5 min before medium change. Cytopathic effect (CPE) was captured after incubation for at least 6 days.

2.9. Statistical Analysis

The primary statistical tests were parametric one-way ANOVA based on three or more repeated test points. Alpha was 0.05. GraphPad Prism version 6.0 software (www.graphpad.com) was used for most analyses. Reported errors are given as standard deviation (SD).

3. Results

Based on the results from cell viability assays and 3D MucilAire Human Nasal Model evaluation, only Formulations C and D were selected for the rest experiments.

3.1. Size Distribution and Zeta Potentials of Particles

As shown in Figure 2, A. FC nanoformulation showed a polydisperse particle size distribution, with a median size of 252.6 + 109 nm (SD, n=2). More than 90% particles are within 222 to 296 nm range, while 6.2% is in 100 nm range. The concentration of particles is 2.2E + 9/ml (2.2 billion particles/ml). For FD nanoformulation (B), a broad particle size was observed, from 45.4 to 331 nm. The median size is 257 + 134 nm (SD, n=2). About 78% particles are in 265 to 331 nm range, and rest were within 45 and 128 nm range. The particle concentration is 6.5E + 9 (6.5 billion/ml). C. The Zeta Potential of FC nanoformulation diluted 30x by water at 25 °C was -29.49 ± 1.02 mV. The Zeta Potential Distribution was 29.49 mV FWHM 6.05 (SL1/2). D. The Zeta Potential of FD nanoformulation diluted 30x by water at 25 °C was -51.31 ± 1.22 mV. The Zeta Potential Distribution was 51.31 mV FWHM 4.47 (SL1/2). These particles appeared to be more evenly distributed in FD compared to FC.

 doi:10.20944/preprints202404.1974.v1

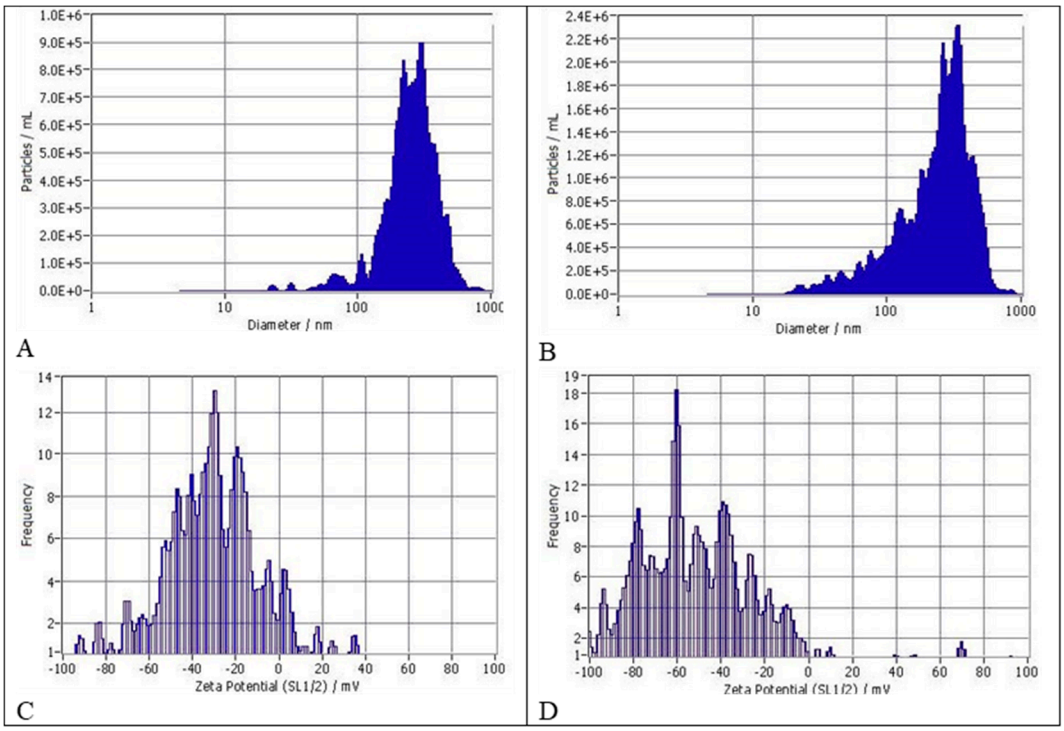

Figure 2. A: Size distribution of particles in FC. B: Size distribution of particles in FD The size distribution profile for one representative sample/formulation determined by NTA is shown. C: Zeta potential and distribution of FC. D. Zeta potential and distribution of FD.

3.2. Cell Viability after 1 h Incubation with HCT-8 Cells

To assess the initial toxicity of the novel EC16m mucoadhesive nanoformulations prior to the 3D Human Nasal Epithelium Model safety tests, the MTT assay was performed on HCT-8 human intestinal epithelial cells after 1 h exposure by the mucoadhesive nasal nanoformulations and overnight incubation. As shown in Figure 3, the untreated control cell viability measured by absorption at wave length 450 nm is 0.843 + 0.105. The value from the vehicle (saline) is 0.784 + 0.014. There is no significant difference between untreated control and saline treated samples (One-Way ANOVA. P=0.32, n=3). Both FA and FB showed significant reduction in MTT values (0.70 + 0.02 and 0.66 + 0.03, respectively) compared to saline (p=0.006 and 0.003, respectively). In contrast, both FC and FD have no significant difference compared to saline treated cells (0.805 + 0.06, p=0.44 and 0.816 + 0.04, p=0.149, respectively).

 doi:10.20944/preprints202404.1974.v1

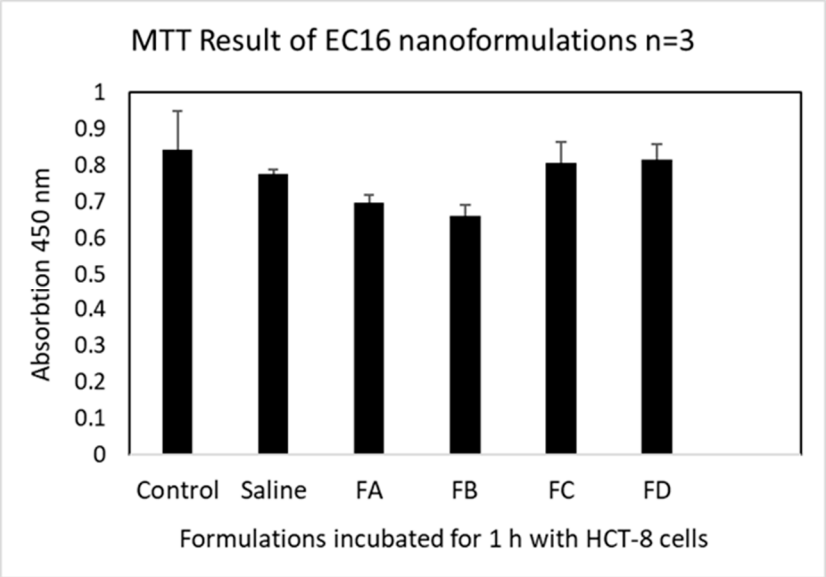

Figure 3. Cell viability (MTT) assay results of the four nanoformulations in comparison to saline as vehicle control. The assay was conducted in 48-well tissue culture plates with confluent HCT-8 cells in each well (n=3).

3.3. Mucociliary Toxicity

3.3.1. Tissue Integrity

The normal range of tissue integrity for MucilAir Human Nasal Epithelium Model are 200-800 Ω.cm2. Figure 4 demonstrates that FC and FD are at the normal range comparable to the untreated control, and FA is below the normal range, while saline and FB are at the lower normal range. Thus, FB, FC, and FD did not impair the tissue integrity.

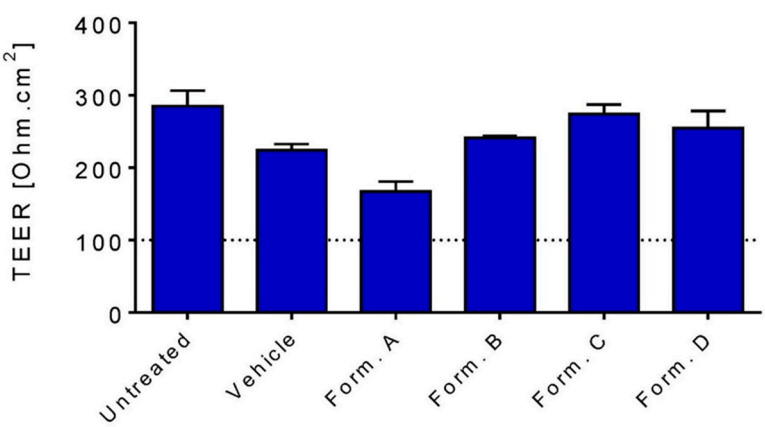

Figure 4. Tissue integrity impact from the nanoformulations in comparison to saline (vehicle).

3.3.2. Cytotoxicity Measured by LDH Release

Results shown in Figure 5 indicate that FA increased LDH release compared to untreated control and vehicle (16% vs. 8%) after twice a day exposure for two days. The other formulations FB, FC and FD did not induce cytotoxicity on LDH release.

 doi:10.20944/preprints202404.1974.v1

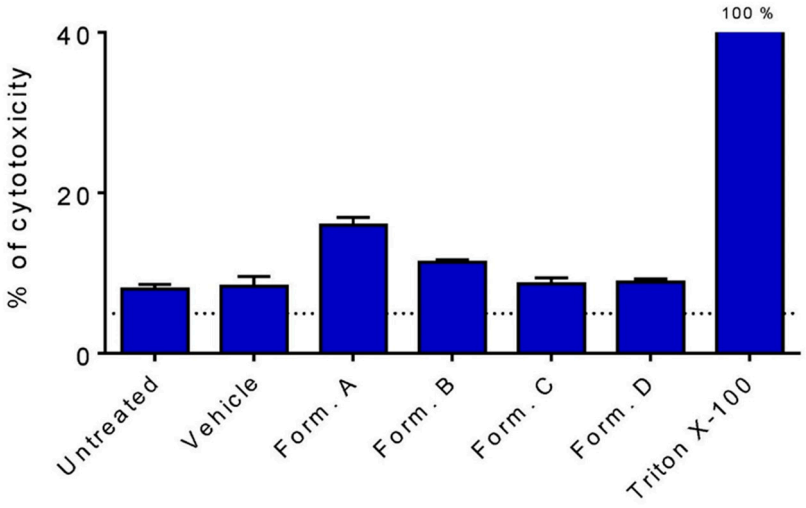

Figure 5. Cytotoxicity induced by the nanoformulations in comparison to untreated control, saline (vehicle), and positive control (10% Triton X-100).

3.3.3. Cilia Beating Frequency (CBF)

After two days exposure of twice a day application of the nanoformulations, the untreated and vehicle controls displayed CBF values of 4,9 and 4,0 Hz (Figure 6). FA significantly reduced the CBF compared to vehicle. FB reduced the CBF slightly but without statistical difference. Both FC and FD showed no significant change compared to vehicle control.

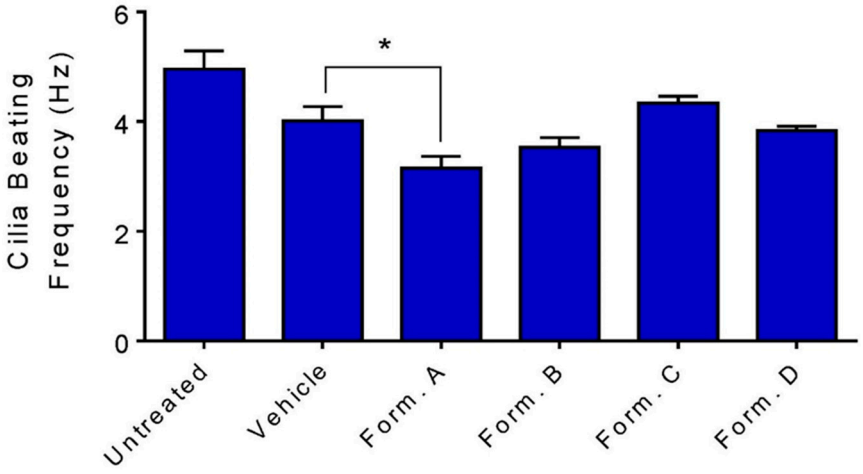

Figure 6. Cilia beating frequency measurements on the four nanoformulations in comparison to saline (vehicle) after two days applications based on twice a day 30 min/each schedule. FA is the only nanoformulation associated with significantly reduced CBF among the formulations.

3.4. Contact Inhibition of OC43 Viral Infectability

According to the results from cell viability and the 3D Human Nasal Epithelium Model safety assessment, FA and FB demonstrated viability and mucociliary safety levels consistently lower than the vehicle (either significant or insignificant), while both FC and FD showed equal levels in the safety parameters compared to the vehicle. Therefore, only FC and FD were used in the in vitro efficacy tests to validate the antiviral activity of the novel mucoadhesive nasal nanoformulations.

As shown in Figure 7, both FC and FD were able to reduce OC43 infectivity by approximately 99.9% ($\log_{10} 3$). The vehicle controls (formulations without EC16m nanoparticles) failed to reduce the

 doi:10.20944/preprints202404.1974.v1

infectivity of the virus. For FC, 5-min and 15-min incubations with the virus led to $\log_{10}$ 3.42 + 0.52 and $\log_{10}$ 3.33 + 0.14 reduction, respectively (p=0.80 One-Way ANOVA). For FD, 5-min and 15-min incubations with the virus led to $\log_{10}$ 2.92 + 0.38 and $\log_{10}$ 2.83 + 0.76 reduction, respectively (p=0.87 One-Way ANOVA). Further statistical calculations indicate there is no statistical differences among incubation time or formulations (One-Way ANOVA, p>0.05).

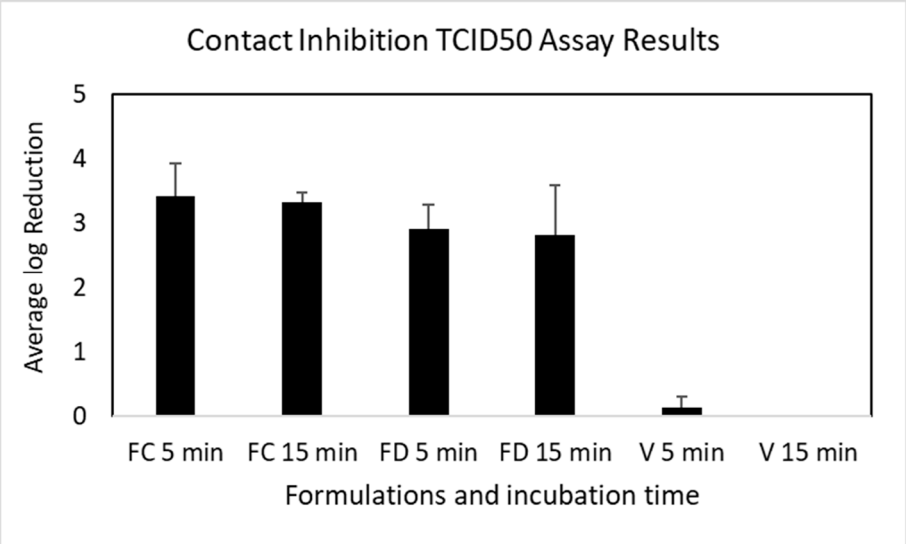

Figure 7. Mean $\log_{10}$ reduction of OC43 infectivity after incubation with FC and FD for 5 and 10 min (V: vehicle controls). The results are from three independent TCID50 assays for the nanoformulations, and two repeated assays for the vehicles. There is no statistical difference among the nanoformulation and incubation time (One-Way ANOVA p>0.05).

3.5. Post-Infection Inhibition of OC43 Viral Replication

As shown in Figure 8, FC nanoformulation exhibited a small inhibitory effect against OC43 replication in MRC-5 cells ($\log_{10}$ 0.83 + 0.14 vs. vehicle control of $\log_{10}$ 0.50 + 0.35) without statistical difference with the vehicle control (p=0.22). In contrast, FD nanoformulation reduced OC43 viral replication by more than 99% ($\log_{10}$ 2.33 + 0.14 vs. vehicle control of $\log_{10}$ 0.5 + 0.353). There is no statistical difference between the vehicle controls.

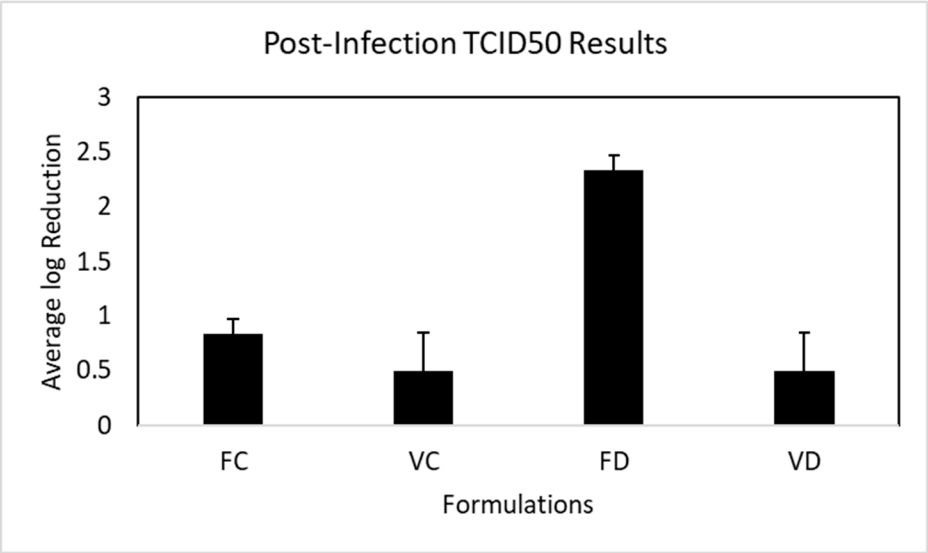

Figure 8. Mean $\log_{10}$ reduction of OC43 infectivity after post-infection incubation with FC and FD for 5 min (VC, VD: vehicle controls for FC and FD, respectively). The results are from three independent

 doi:10.20944/preprints202404.1974.v1

TCID50 assays for the nanoformulations, and two repeated assays for the vehicles. There is a significant difference between FC and FD nanoformulations (One-Way ANOVA p=0.001). There is no statistical difference between FC and its vehicle (One-Way ANOVA p=0.22).

4. Discussion

The current study is the first attempt to validate the suitability of EC16m nanoparticle/saline based mucoadhesive nasal formulations using 3D MucilAir Human Nasal Epithelium Model (MucilAir) and in vitro toxicity/efficacy methods. We previously reported a series test results from EC16 and EC16m nanoformulations, which are from saline-based aqueous suspensions of the nanoparticles such as F18, F18D, F18m and F18Dm [8,9]. These high efficacy nanoformulations lack the mucoadhesive nature, therefore are not suitable for nasal application due to the mucociliary clearance transit time of 20 min [39]. Accordingly, the novel nanoformulations tested in the current study were adjusted with the addition of CMC to increase the viscosity up to 19 mPa, which increased the mucoadhesive capability and the mucociliary clearance time. With a pH at approximately 6.20, the FC and FD formulations are comparable to that of human nasal cavity.

Compared to EC16 nanoparticles such as F18D [9], the EC16m nanoparticles FC and FD have a slightly larger particle size. As shown in Figure 2, Nanoparticles in FC have a median size of 252.6 + 109 nm (SD, n=2), and nanoparticles in FD have a median size is 257 + 134 nm (SD, n=2). In contrast, the F18D particles have a median particle size was 186.6 + 20.62 nm [9]. This difference could be due to the chemical and physical differences between EC16m (EGCG-mono-palmitate) and EC16 (EGCG-palmitates containing 50% EC16m), which is a mixture of EGCG-mono-palmitate, EGCG-di-palmitate, and EGCG-tri-palmitates [42]. Comparing FC and FD, the particle density of FD is 3 times more than FC, which is reflected from the more polydisperse particle size in FD (more smaller particles) (Figure 2). The addition of the food-grade dispersing agent in FD also resulted in a greater Zeta potential (-51.31 ± 1.22 mV) than FC nanoformulation (-29.49 ± 1.02 mV), suggesting FD nanoformulation is more stable (Figure 2). Thus, the dispersing agent plays an important role for FD formulation's stability by preventing particle aggregation. On the other hand, the direct contact antiviral activities between the two nanoformulations are comparable without statistical difference (Figure 7).

The results from MTT assays and the 3D Human Nasal Epithelium Model demonstrate both FC and FD nanoformulations showed comparable levels in cytotoxicity and mucociliary toxicity with the vehicle (saline) control (Figures 3–6). Normal saline (0.9% NaCl) is used widely in nasal formulations with a consistent safety record [43]. The current toxicity data of FC and FD confirmed that these mucoadhesive nasal nanoformulations are tolerable by human nasal epithelium without acute toxicity.

As shown in Figure 7, the saline-based vehicles have no antiviral activity on OC43 virus, while both FC and FD nanoformulations possess potent antiviral activity at concentration range of 0.005 (70 μM) to 0.02% (280 μM). This concentration range is significantly lower than F18D nanoformulation containing EC16 particles (0.1% or 1.25 mm) [9]. The F18D nanoformulation is extremely active against OC43 with a one min time-kill rate of 99.9999% [9]. However, A 3D Human Nasal Epithelium Model test indicates the F18D nanoformulation is toxic to the nasal epithelium (data not shown). It is interesting to observe that all of the EC16 or EC16m nanoformulations tested so far demonstrated a rapid action against human coronavirus [8,9]. This rapid antiviral action is also seen in FC and FD, where 5-min and 15-min incubations with OC43 virus did not have significant difference in efficacy (Figure 7), suggesting the damage of the viral structure occurred immediately upon contact with the formulations, as we reported previously [9].

Unlike the results from the contact time-kill assays, where both FC and FD exhibited potent antiviral activity. A surprising result from post-infection inhibition assay was observed, which indicates that FC has little effectiveness against OC43 viral replication after the virus already entered the cells (Figure 8). One explanation could be the difference in particle size distribution between the two nanoformulations. Only 6.2% of FC nanoparticles are in 100 nm range, while 93.8% of particles are in 200 to 300 nm range (Figure 1A). In contrast, 78.3% particles in FD are in 200 to 330 nm range,

 doi:10.20944/preprints202404.1974.v1

and the rest (21.7%) are in 45 to 124 nm range (Figure 1B). It could be postulated that smaller particles enter the cells in higher efficiency than larger particles, therefore the FD nanoformulation shows a significantly higher antiviral effect (>99%) (Figure 8). This particle size associated intracellular antiviral activity should be further explored, which would be important for new drug designs. Another factor that cannot be ruled out is the presence of CMC, which increased the viscosity of the nanoformulation. That is, the large particles in FC formulation may have a slower release from a thick formulation onto the cell membrane within 5 min.

According to the pathogenesis of Long COVID, an ideal intranasal intervention targeting the cause of Long COVID neurologic symptoms should contain an agent (drug) possessing a potent antiviral activity to clear the persistent viral presence; a strong anti-inflammatory property to reduce inflammation in the affected tissues; and a powerful antioxidant activity. In addition, the formulation must be safe and stable. Based on the overall considerations, Formulation D (FD) is the best EC16m nanoformulation for this purpose due to the efficacy (>99% reduction of viral infectivity in direct contact or post-infection application in 5 min), mucociliary safety (similar to Normal saline), and stability (Zeta potential at -50 mV). There are several advantages of the patent-pending "facilitated self-assembled" EGCG-mono-palmitate nanoparticles (EC16m) over other EGCG nanoparticles. One of the advantages is the amphipathic chemical nature of EC16m, which not only significantly increased the antiviral activity against human pathogenic viruses, but also increased the bioavailability to reach target tissues. Quantitatively, the particle density of FD is 6.5 billion particles/ml. In general, a full nasal spray volume is approximately 0.07 ml. Therefore, each spray of FD nanoformulation delivers 455 million EC16m nanoparticles. Since the persistent infection of the olfactory mucosa is associated with >0.5 million RNA copies [44] (not the number of viable viral particles), on a proportional basis, 0.07 ml/nostril (0.14) of FD nanoformulation (910 million nanoparticles) would be sufficient to inactivate (by structural change and other mechanisms) the coronavirus in the olfactory mucosa within a short period of time. In addition, a small portion of the EC16m nanoparticles will enter the CNS prior to cilia clearance and release free EGCG to perform anti-inflammatory, antioxidant and neuroprotective activities.

In summary, the results of the current study demonstrated that the saline-based EC16m mucoadhesive nasal Formulation D is highly effective against human β-coronavirus OC43, the strain with high genome homology with SARS-CoV-2 (45), and in reducing viral replication after a single 5-min post-infection treatment, without mucociliary toxicity. With the known anti-inflammatory, antioxidant, and neuroprotective properties, intranasally delivered EC16m by Formulation D could not only terminate the "persistent infection" in the olfactory epithelium, but also inhibit local inflammation and apoptosis, thereby restore the olfactory function and reduce free radical levels and inflammation in the CNS.

5. Conclusions

In conclusion, an EC16m (drug grade) intranasal nanoformulation D is suitable for a new intranasal drug to minimize Long COVID-associated anosmia and other neurologic symptoms, pending chronic mucociliary safety and human studies.

6. Patents

PCT/US23/74377 Pending: Compositions and methods of minimizing Long CPVID. Inventor: Stephen Hsu (2023).

Author Contributions: Conceptualization, S.H., D.D.; methodology, N.F., G.L., and X.J.; Zeta View validation, Y.L., H.Y., J.C. and D.D.; formulation data analysis, S.H., H.Y, J.C.; investigation, N.F., D.D., and S.H.; resources, Y.L.; data curation, S.H.; EC16m analysis, B.Y and X.J.; writing—original draft preparation, S.H.; writing—review and editing, D.D.; visualization, N.F.; supervision, S.H. and D.D.; project administration, S.H.; funding acquisition, S.H., D.D. All authors have read and agreed to the published version of the manuscript.

Funding: This work was funded by a grant from the National Institute on Deafness and Other Communication Disorders (NIDCD) (1R41DC020678-01). The content is solely the responsibility of the authors and does not necessarily represent the official views of the National Institutes of Health.

 doi:10.20944/preprints202404.1974.v1

Institutional Review Board Statement: NA

Informed Consent Statement: NA

Acknowledgments: The authors want to thank Epithelix Sàrl for mucociliary toxicity evaluations, and support from Augusta University Research Institute and Office of Innovation Commercialization.

Appendix A

Detailed original ZetaView results shown in Figure 2.

Appendix B

Protocols of Epithelix Sarl's 3D Human Nasal Epithelium Model evaluation of the nanoformulation samples.

References

1. Leonel, J.W.; Ciurleo, G.C.V.; Formiga, A.M.; et al. Long COVID: neurological manifestations - an updated narrative review. *Dement. Neuropsychol*. **2024**, *18*, DOI: 10.1590/1980-5764
2. Stefanou M.I., Palaiodimou L., Bakola E., et al. Neurological manifestations of long-COVID syndrome: a narrative review. *Ther Adv Chronic Dis.* **2022**, *13*, DOI: 10.1177/20406223221076890.
3. Groff, D.; Sun, A.; Ssentongo, A.E; et al. Short-term and Long-term Rates of Postacute Sequelae of SARS-CoV-2 Infection: A Systematic Review. *JAMA Netw Open.* **2021**, *4*, DOI: 10.1001/jamanetworkopen.2021.28568.
4. Leng, A.; Shah, M.; Ahmad, S.A.; et al. Pathogenesis Underlying Neurological Manifestations of Long COVID Syndrome and Potential Therapeutics. *Cells*. **2023,** *12*, DOI: 10.3390/cells12050816.
5. Abdelalim, A.A.; Mohamady, A.A.; Elsayed, R.A.; Elawady, M.A.; Ghallab, A.F. Corticosteroid nasal spray for recovery of smell sensation in COVID-19 patients: A randomized controlled trial. *Am. J. Otolaryngol.* **2021**, *42*, DOI: 102884.
6. Gupta, S.; Lee, J.J.; Perrin, A.; Khan, A.; Smith, H.J.; Farrell, N.; Kallogjeri, D.; Piccirillo, J.F. Efficacy and Safety of Saline Nasal Irrigation Plus Theophylline for Treatment of COVID-19-Related Olfactory Dysfunction: The SCENT2 Phase 2 Randomized Clinical Trial. *JAMA Otolaryngol Head Neck Surg*. **2022**, *148*, 830-837; DOI: 10.1001/jamaoto.2022.1573.
7. Najafloo, R.; Majidi, J.; Asghari, A.; Aleemardani, M.; Kamrava, S.K.; Simorgh, S.; Seifalian, A.; Bagher, Z.; Seifalian. A.M. Mechanism of Anosmia Caused by Symptoms of COVID-19 and Emerging Treatments. *ACS Chem Neurosci*. **2021**, *12*, 3795-3805, DOI: 10.1021/acschemneuro.1c00477.
8. Frank, N.; Dickinson, D.; Garcia, W.; Xiao, L.; Xayaraj, A.; Lee, L.H.; Chu, T.; Kumar, M.; Stone, S.; Liu, Y.; Yu, H.; Cai, J.; Yao, B.; Jiang, X.; Hsu, S. Evaluation of Aqueous Nanoformulations of Epigallocatechin-3-Gallate-Palmitate (EC16) Against Human Coronavirus as a Potential Intervention Drug. *Biomed J Sci & Tech Res.* **2023**, *50*, DOI: 10.26717.
9. Frank, N.; Dickinson, D.; Garcia, W.; Liu, Y.; Yu, H.; Cai, J.; Patel, S.; Yao, B.; Jiang, X.; Hsu, S. Feasibility Study of Developing a Saline-Based Antiviral Nanoformulation Containing Lipid-Soluble EGCG: A Potential Nasal Drug to Treat Long COVID. *Viruses*. **2024**, *16*, 196, DOI: 10.3390/v16020196.
10. Dinda, B.; Dinda, S.; Dinda, M. Therapeutic potential of green tea catechin, (-)-epigallocatechin-3-O-gallate (EGCG) in SARS-CoV-2 infection: Major interactions with host/virus proteases. *Phytomed Plus.* **2023**, *3*, DOI: 10.1016/j.phyplu.2022.100402.
11. Hsu, S. Compounds Derived from Epigallocatechin-3-Gallate (EGCG) as a Novel Approach to the Prevention of Viral Infections. *Inflamm Allergy Drug Targets*. **2015**, *14*, 13-18, DOI: 10.2174/1871528114666151022150122.
12. Hurst, B.L.; Dickinson, D.; Hsu, S. Epigallocatechin-3-Gallate (EGCG) Inhibits SARS-CoV-2 Infection in Primate Epithelial Cells: (A Short Communication). *Microbiol Infect Dis*. **2021**, *5*, 1-6, DOI: 10.33425/2639-9458.1116.
13. Chen, P.; Dickinson, D.; Hsu, S. Lipid-soluble Green Tea Polyphenols: Stabilized for Effective Formulation. In *Handbook of Green Tea and Health Research*. McKinley, H., Jamieson, M., Eds.; Nova Science Publishers, Inc.: New York, 2009; pp. 45-61.
14. Hsu, S.; Dickinson, D. Green tea and skin protection: Mechanism of action and practical applications. *Household and Personal Care. TODAY* **2009**, *2*, 33-36, DOI: 10.1016/j.jaad.2004.12.044.

15. Liu, B.; Kang, Z.; Yan, W. Synthesis, Stability, and Antidiabetic Activity Evaluation of (−)-Epigallo-catechin Gallate (EGCG) Palmitate Derived from Natural Tea Polyphenols. *Molecules*. **2021**, *26*, 393, DOI: 10.3390/molecules26020393.
16. Hsu, S.; Dickinson, D.; Borke, J.; Walsh, D.S.; Wood, J.; Qin, H.; Winger, J.; Pearl, H.; Schuster, G.; Bollag, W.B. Green tea polyphenol induces caspase 14 in epidermal keratinocytes via MAPK pathways and reduces psoriasiform lesions in the flaky skin mouse model. *Experimental Dermatology*. **2007**, 16, 678–684, DOI: 10.1111/j.1600-0625.2007.00585.x.
17. Gillespie, K.; Kodani, I.; Dickinson, D.P.; Ogbureke, K.U.E.; Camba, A.M.; Wu, M.; Looney, S.; Chu, T.C.; Qin, H.; Bisch, F.; Sharawy, M.; Schuster, G.S.; Hsu. S.D. Effects of oral consumption of the green tea polyphenol EGCG in a murine model for human Sjogren's syndrome, an autoimmune disease. *Life Sciences*. **2008**, *83*, 581–588, DOI: 10.1016/j.lfs.2008.08.011.
18. Hsu, S.D.; Dickinson, D.P.; Qin, H.; Borke, J.; Ogbureke, K.U.E.; Winger, J.N.; Camba, A.M.; Bollag, W.B.; Stöppler, H.J.; Sharawy, M.M.; Schuster, G.S. Green tea polyphenols reduce autoimmune symptoms in a murine model for human Sjogren's syndrome and protect human salivary acinar cells from TNF-alpha-induced cytotoxicity. *Autoimmunity*. **2007**, *40*, 138-47, DOI: 10.1080/08916930601167343.
19. Dickinson, D.; DeRossi, S.; Yu, H.; Thomas, C.; Kragor, C.; Paquin, B.; Hahn, E.; Ohno, S.; Yamamoto, T.; Hsu, S. Epigallocatechin-3-gallate modulates antioxidant defense enzyme expression in murine submandibular and pancreatic exocrine gland cells and human HSG cells. *Autoimmunity*. **2014**, *47*, 177–184, DOI: 10.3109/08916934.2013.879470.
20. Dickinson, D.; Yu, H.; Ohno, S.; Thomas, C.; Derossi, S.; Ma, Y.H.; Yates, N.; Hahn, E.; Bisch, F.; Yamamoto, T.; Hsu, S. Epigallocatechin-3-gallate prevents autoimmune-associated down- regulation of p21 in salivary gland cells through a p53-independent pathway. *Inflamm Allergy Drug Targets*. **2014**, *13*, 15-24, DOI: 10.2174/1871528112666131211102500.
21. de la Torre, R.; de Sola, S.; Farre, M.; Xicota, L.; Cuenca-Royo, A.; Rodriguez, J.; Leon, A.; Langohr, K.; Gomis-Gonzalez, M.; Hernandez, G.; et al. A phase 1, randomized double-blind, placebo controlled trial to evaluate safety and efficacy of epigallocatechin-3-gallate and cognitive training in adults with Fragile X syndrome. *Clin Nutr*. **2020**, *39*, 378-387. DOI: 10.1016/j.clnu.2019.02.028.
22. Singh, N.A.; Mandal, A.K.; Khan, Z.A. Potential neuroprotective properties of epigallocatechin-3-gallate (EGCG). *Nutr J*. **2016**, *15*, 60, DOI:10.1186/s12937-016-0179-4.
23. Cano, A.; Ettcheto, M.; Espina, M.; Auladell, C.; Calpena, A.C.; Folch, J.; Barenys, M.; Sánchez-López, E.; Camins, A.; García, M.L. Epigallocatechin-3-gallate loaded PEGylated-PLGA nanoparticles: A new anti-seizure strategy for temporal lobe epilepsy. *Nanomedicine: Nanotechnology, Biology and Medicine*. **2018**, *14*, 1073-1085, DOI: 10.1016/j.nano.2018.01.019.
24. Cai, Z.Y.; Li, X.M.; Liang, J.P.; Xiang, L.P.; Wang, K.R.; Shi, Y.L.; Yang, R.; Shi, M.; Ye, J.H.; Lu, J.L.; et al. Bioavailability of Tea Catechins and Its Improvement. *Molecules*. **2018**, *23*, 2346, DOI: 10.3390/molecules23092346.
25. Yang, C.S.; Chen, L.; Lee, M.J.; Balentine, D.; Kuo, M.C.; Schantz, S.P. Blood and urine levels of tea catechins after ingestion of different amounts of green tea by human volunteers. *Cancer Epidemiol Biomarkers Prev*. **1998**, *7*, 351-354, PMID: 9568793.
26. Zhong, J.; Dickinson, D.; Sampath, L.; Hsu, S. Effects of Epigallocatechin-3-Gallate-Palmitate (EC16) on In Vitro Norovirus Infection. *Microbiol Infect Dis*. **2021**, *5*, 1-7, DOI: 10.33425/2639-9458.1139.
27. Wei, Y., Chen, P., Ling, T., Wang, Y., Dong, R., Zhang, C., Zhang, L., Han, M., Wang, D., Wan, X., & Zhang, J. Certain (-)-epigallocatechin-3-gallate (EGCG) auto-oxidation products (EAOPs) retain the cytotoxic activities of EGCG. *Food Chem*. **2016**, *204*, 218–226, DOI: 10.1016/j.foodchem.2016.02.134.
28. de Oliveira, A.; Adams, S.D.; Lee, L.H.; Murray, S.R.; Hsu, S.D.; Hammond, J.R.; Dickinson, D.; Chen, P.; Chu, T.C. Inhibition of herpes simplex virus type 1 with the modified green tea polyphenol palmitoyl-epigallocatechin gallate. *Food Chem Toxicol*. **2013**, *52*, 207-215, DOI: 10.1016/j.fct.2012.11.006.
29. Mori, S.; Miyake, S.; Kobe, T.; Nakaya, T.; Fuller, S.D.; Kato, N.; Kaihatsu, K. Enhanced anti-influenza A virus activity of (-)-epigallocatechin-3-O-gallate fatty acid monoester derivatives: effect of alkyl chain length. *Bioorg Med Chem Lett*. **2008**, *18*, 4249-4252, DOI: 10.1016/j.bmcl.2008.02.020.
30. Barhoum, A.; García-Betancourt, M.L.; Jeevanandam, J.; Hussien, E.A.; Mekkawy, S.A.; Mostafa, M.; Omran, M.M.; Abdalla, M.S.; Bechelany, M. Review on Natural, Incidental, Bioinspired, and Engineered Nanomaterials: History, Definitions, Classifications, Synthesis, Properties, Market, Toxicities, Risks, and Regulations. *Nanomaterials (Basel)*. **2022**, *12*, 177, DOI: 10.3390/nano12020177.

31. Farabegoli, F.; Granja, A.; Magalhães, J.; Purgato, S.; Voltattorni, M.; Pinheiro, M. Epigallocatechin-3-gallate Delivered in Nanoparticles Increases Cytotoxicity in Three Breast Carcinoma Cell Lines. *ACS Omega*. **2022**, *7*, 41872–41881, DOI: 10.1021/acsomega.2c01829.
32. Farabegoli, F.; Pinheiro, M. Epigallocatechin-3-Gallate Delivery in Lipid-Based Nanoparticles: Potentiality and Perspectives for Future Applications in Cancer Chemoprevention and Therapy. *Front Pharmacol*. **2022,** *13*, DOI: 10.3389/fphar.2022.809706.
33. Chen, B.H.; Hsieh, C.H.; Tsai, S.Y.; Wang, C.Y.; Wang, C.C. Anticancer effects of epigallocatechin-3-gallate nanoemulsion on lung cancer cells through the activation of AMP-activated protein kinase signaling pathway. *Sci Rep.* **2020**, *10*, DOI: 10.1038/s41598-020-62136-2.
34. He, A.; Guan, X.; Song, H.; Li, S.; Huang, K. Encapsulation of (−)-epigallocatechin-gallate (EGCG) in hordein nanoparticles. *Food Bioscience*. **2020**, *37*, DOI: 100727.34.
35. Song, H.; He, A.; Guan, X.; Chen, Z.; Bao, Y.; Huang, K. Fabrication of chitosan-coated epigallocatechin-3-gallate (EGCG)-hordein nanoparticles and their transcellular permeability in Caco-2/HT29 cocultures. *Int J Biol Macromol*. **2022**, *196*, 144-150, DOI: 10.1016/j.ijbiomac.2021.12.024.
36. Jiang, Y.; Jiang, Z.; Ma, L.; Huang, Q. Advances in Nanodelivery of Green Tea Catechins to Enhance the Anticancer Activity. *Molecules*. **2021**, *26*, DOI: 10.3390/molecules26113301.
37. Krzyzowska, M.; Janicka, M.; Chodkowski, M.; Patrycy, M.; Obuch-Woszczatyńska, O.; Tomaszewska, E.; Ranoszek-Soliwoda, K.; Celichowski G.; Grobelny, J. Epigallocatechin Gallate-Modified Silver Nanoparticles Show Antiviral Activity against Herpes Simplex Type 1 and 2. *Viruses*. **2023**, 15, DOI: 10.3390/v15102024.
38. Meesaragandla, B.; Hayet, S.; Fine, T.; Janke, U.; Chai, L.; Delcea, M. Inhibitory Effect of Epigallocatechin Gallate-Silver Nanoparticles and Their Lysozyme Bioconjugates on Biofilm Formation and Cytotoxicity. *ACS Appl Bio Mater*. **2022**, *5*, 4213–4221, DOI: 10.1021/acsabm.2c00409.
39. Sakakura, Y., Ukai, K., Majima, Y., Murai, S., Harada, T., & Miyoshi, Y. Nasal mucociliary clearance under various conditions. *Acta Otolaryngol*. **1983**, *96*, 167–173, DOI:10.3109/00016488309132888.
40. Helwa, I.; Cai, J.; Drewry, M.D.; et al. A Comparative Study of Serum Exosome Isolation Using Differential Ultracentrifugation and Three Commercial Reagents. *PLoS One.* 2017, *12*, DOI: 10.1371/journal.pone.0170628.
41. Reed, L.J.; Muench, H.; A simple method of estimating 50 percent end points. *Am. J. Hyg.* **1938**, *27*, 493-497.
42. US FDA GRAS NOTICE 772, U.G.N. GRAS Notice for Oil-Soluble Green Tea Extract (Green Tea Catechin Palmitate). **2018**. (Chrome-extension://efaidnbmnnnibpcajpcglclefindmkaj/https://www.fda.gov/media/126906/download)
43. Rabago, D.; Zgierska, A. Saline nasal irrigation for upper respiratory conditions. *Am Fam Physician.* **2009**, *80*, 1117-9, PMID: 19904896.
44. de Melo, G.D.; Lazarini, F.; Levallois, S.; Hautefort, C.; Michel, V.; Larrous, F.; Verillaud, B.; Aparicio, C.; Wagner, S.; Gheusi, G.; et al. COVID-19-related anosmia is associated with viral persistence and inflammation in human olfactory epithelium and brain infection in hamsters. *Sci Transl Med*. **2021**, *13*, DOI: 10.1126/scitranslmed.abf8396.
45. Kim, M.I.; Lee, C. Human Coronavirus OC43 as a Low-Risk Model to Study COVID-19. *Viruses*. **2023**, *15*, DOI: 10.3390/v15020578.